Strain actuation of barium titanate single crystals under electromechanical loading in the non-polar [110] direction

2013 Smart Mater. Struct. 22 094011

(http://iopscience.iop.org/0964-1726/22/9/094011)

IOP PUBLISHING SMART MATERIALS AND STRUCTURES

Smart Mater. Struct. **22** (2013) 094011 (10pp) doi:10.1088/0964-1726/22/9/094011

Strain actuation of barium titanate single crystals under electromechanical loading in the non-polar [110] direction

Jay Shieh[1], Yen-Nan Lin[1], Nien-Ti Tsou[2] and Yi-Chung Shu[3]

[1] Department of Materials Science and Engineering, National Taiwan University, Taipei 106, Taiwan
[2] Department of Engineering Science, University of Oxford, Oxford OX1 3PJ, UK
[3] Institute of Applied Mechanics, National Taiwan University, Taipei 106, Taiwan

E-mail: jayshieh@ntu.edu.tw

Received 13 January 2013, in final form 25 March 2013
Published 27 August 2013
Online at stacks.iop.org/SMS/22/094011

Abstract

The switching characteristics of $BaTiO_3$ single crystals subjected to uniaxial electromechanical loading in the non-polar [110] direction at room temperature and 55 °C were investigated. Polarization and strain hysteresis measurements in the [110] direction revealed that under the combination of large in-plane switching coercivities and a strong out-of-plane depolarization field (induced by the shape irregularity and large unshielded surfaces of the crystal sample), strain-inducing 90° in-plane to out-of-plane (or vice versa) switching was the dominant switching behavior even in the absence of mechanical bias. By lowering the in-plane switching coercivities, which was achieved by increasing the loading temperature from room temperature to 55 °C, a contrasting non-strain-inducing switching behavior characterized by 90° and/or 180° switches between the in-plane variants was observed instead. The contrasting switching behavior at two different temperatures indicates that apart from the bias stress magnitude, the combined effect of the depolarization field and switching coercivity is another critical factor governing the strain actuation of $BaTiO_3$ single crystals. The [110] electromechanical loading responses reveal the possibility of increasing the strain capacity of $BaTiO_3$ single crystals by introducing accompanying depolarization fields which promote strain-inducing 90° switching. Such an approach could be potentially useful when bias stress-activated ferroelastic switching is not attainable.

(Some figures may appear in colour only in the online journal)

1. Introduction

Recent attempts to develop large strain actuation in tetragonal barium titanate ($BaTiO_3$) single crystals have focused on inducing ferroelastic 90° domain switching through electromechanical loading in one of the crystal's polar (or variant) directions [1–6]. Here, the phrase 'polar directions' means the equivalent crystallographic directions (i.e., six ⟨100⟩ directions) which the polarization can adopt. Several important conclusions were drawn from these studies: (1) the magnitude of electrostrain produced is strongly dependent on the bias stress level (i.e., extent of stress-activated ferroelastic switching) [1, 2]; (2) strain capacity is significantly increased for $BaTiO_3$ single crystals exhibiting small 180° switching coercivities [2, 3]; and (3) decoupling between switching strain and switching polarization during electric field unloading is likely to be caused by the cooperative operation of multiple 90° switching systems under mechanical bias [4]. Despite the number of studies detailing the electromechanical switching in $BaTiO_3$ single crystals, the polarization and strain responses of the crystals under electromechanical loading in the crystal's non-polar directions have not been discussed in the existing literature. As for large electric field loading in the non-polar directions, several well-known studies have documented the electric-field-induced phase transformation and engineered domain configurations of

$BaTiO_3$ and lead zinc (or magnesium) niobate–lead titanate (PZN-PT, PMN-PT) single crystals [7–10].

The aim of the present study is to investigate the polarization and strain responses of (001)-oriented $BaTiO_3$ single crystals under uniaxial electromechanical loading in the non-polar [110] direction at room temperature and 55 °C. This is to shed insight into the selection of the switching route in ferroelectric single crystals when subjected to electromechanical loading in a non-polar direction. How much strain a ferroelectric single crystal can produce under a specific electromechanical loading condition is critically dependent on the switching route taken by the domains. The notion of misalignment between the loading and polar directions is strongly relevant to the application of bulk ferroelectric single crystals, since difficulties encountered in crystal processing and cutting may limit the crystal orientations available for load application. Besides the bias stress magnitude, other factors which might influence the electrostrain of $BaTiO_3$ single crystals, such as the switching coercivity and domain wall mobility, are examined in this study by changing the loading temperature. At 55 °C, which is well below the ferroelectric–paraelectric Curie temperature (T_c) of $BaTiO_3$ (T_c = 120–130 °C), while a large polarization remains attainable through domain switching, the switching characteristics of $BaTiO_3$ single crystals are notably different to those observed at room temperature, due to the additional thermal energy [5]. The spontaneous polarization of $BaTiO_3$ single crystals extrapolated at 55 °C by Merz [11] was 0.237 C m^{-2}, approximately 91% of the room temperature value. However, recent loading studies on $BaTiO_3$ single crystals have shown contrary measurements where larger remanent and saturation polarizations were observed at 55 °C due to incomplete polarization switching at room temperature [4, 5].

2. Materials and methods

2.1. Electromechanical loading

Polarization and strain hysteresis measurements under combined uniaxial electrical and mechanical loading were performed on unpoled (001)-oriented cuboidal $BaTiO_3$ single crystals, measuring 5 × 5 × 2 mm^3, in the [110] direction at room temperature and 55 °C. This was achieved by machining the square cuboid crystal into a hexagonal prism by cutting off two opposite corners of the cuboid, and the resulting two parallel cut faces became the top and bottom electrode surfaces to allow the application of electrical and mechanical loads parallel to the [110] direction of the crystal (i.e., perpendicular to the [001] and at 45° to the [100] and [010] directions). The geometry and optical image of the hexagonal prism crystal sample, together with the laboratory coordinate system and definition of the loading, in-plane and out-of-plane directions are shown in figure 1—the laboratory +3 direction is the [110] direction of the crystal sample. Miniature strain gauges (FBX-04-11-005LE, TML, Japan) were attached onto the hexagonal side faces of the crystal sample to measure strain changes in the [110] direction. A

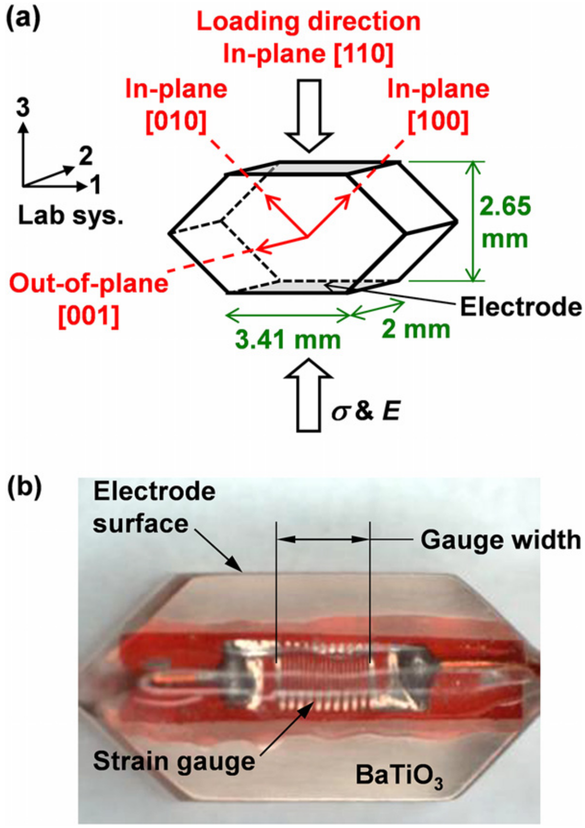

Figure 1. (a) Geometry and (b) optical image of a hexagonal prism shape $BaTiO_3$ single crystal sample prepared for [110] electromechanical loading experiments. The laboratory coordinate system and loading, in-plane and out-of-plane directions are defined in (a).

thin coat of epoxy resin was applied to the exposed surface of the strain gauges to afford extra insulation against electrical breakdown. The length of the hexagonal prism crystal sample was longer than that of the electrodes (see figure 1(a)); however, the two triangular flanks of the crystal sample were not cut off in order to provide enough surface area for strain gauge attachment. The active grid (gauge) width of the miniature strain gauges (1.3 mm) was much shorter than the length of the electrodes (see figure 1(b)); this allowed accurate strain sensing of the central portion of the hexagonal prism crystal sample, which experienced relatively uniform electrical and mechanical loads at any instant of the loading process.

The unpoled (001)-oriented $BaTiO_3$ single crystals used in this study were obtained from MTI Co., CA, USA. The electromechanical loading fixture and the heating and measuring apparatuses were identical to the ones reported in the authors' previous studies [5, 12]. Cyclic electrical loading was supplied by a high-voltage amplifier (20/20C, Trek, USA) in the form of a sinusoidal electric field of amplitude ±1.25 MV m^{-1} and frequency 0.2 Hz. A ferroelectric analyzer (TF2000, aixACCT, Germany) was used for charge measurement. Mechanical loading was supplied by a universal testing machine (HT-9102, Hung-Ta, Taiwan) in the form of a series of compressive stresses (up to 17 MPa) applied

Table 1. Material parameters of tetragonal single crystal $BaTiO_3$ with [001] polarization, where c_{pq} is the stiffness matrix ($p, q = 1$–6), κ_{ij} is the permittivity matrix ($i, j = 1$–3) under constant strain, and e_{ip} is the matrix of piezoelectric coefficients [13, 14].

c_{11}	275×10^9 Pa	c_{12}	179×10^9 Pa	c_{13}	152×10^9 Pa
c_{33}	165×10^9 Pa	c_{44}	54.3×10^9 Pa	c_{66}	113×10^9 Pa
e_{15}	21.3 C m^{-2}	e_{31}	-2.69 C m^{-2}	e_{33}	3.65 C m^{-2}
κ_{11}	1.74×10^{-8} F m^{-1}	κ_{33}	9.65×10^{-10} F m^{-1}		

constantly in the [110] direction. The entire loading fixture was supported in a heatable silicon oil bath to prevent breakdown arcing. Heating of the oil bath was provided by a digitally controlled resistive heating element suspended within the oil. The temperatures of different regions within the oil bath were monitored by thermocouples.

2.2. Finite element analysis

The influence of the hexagonal prism shape on the distributions of electric potential, stress and displacement vectors within the crystal sample was examined by the finite element (FE) method. Two types of variant configurations in the crystal sample were adopted when performing FE simulations: (1) the presence of only the out-of-plane [001] and [00$\bar{1}$] variants and (2) the presence of only the in-plane [100] and [010] variants. These two variant configurations could be associated with the polarization saturation states induced by a large [110] compressive stress and a large [110] electric field, respectively. The FE simulations performed were static simulations, in which no ferroelectric or ferroelastic switching occurred within the crystal sample. Ten-node tetrahedral elements were adopted for three-dimensional simulations and each element represented a single ferroelectric variant. Quadratic shape functions were used to describe the displacement and electric field at each node in terms of the nodal displacements u_i and scalar electric potential ϕ. Nodal stress was obtained by averaging the stresses on the neighboring Gauss points. The material properties of tetragonal single crystal $BaTiO_3$ with polarization along the [001] direction were used in the FE calculations and are listed in table 1 [13, 14]. These properties were treated as the properties of the [001] ferroelectric variant. While for other ferroelectric variants, their properties were determined from pure rotation by 90° and 180°, according to their relative orientation.

The mesh arrangement and boundary conditions assigned to the hexagonal prism crystal sample are shown in figure 2. The mesh has an average element edge length of 0.1 mm. To construct the above-mentioned two types of variant configurations, the material properties of the two variants present in each configuration (i.e., [001] and [00$\bar{1}$] pair or [100] and [010] pair) were randomly assigned to all elements without considering compatibility. The displacements along the 3-axis of the nodes at the top surface u_3^{T} and bottom surface u_3^{B} of the sample were set such that $u_3^{\mathrm{T}} = s_{33}^{*}\sigma_3 h$ and $u_3^{\mathrm{B}} = 0$, where s_{33}^{*} is the effective compliance coefficient along the 3-axis (i.e., the average of the compliance coefficients of the two variants present in the sample), σ_3 is the applied compressive stress along the 3-axis, and h is the height of the sample (2.65×10^{-3} m). The stress-dependent uniform displacement of the top surface nodes (in the −3 direction) was set up to imitate the application of compressive stress in the actual loading scenario, where the top surface of the hexagonal prism crystal sample was compressed by the flat surface loading platen of the universal testing machine. The electric potential applied to the nodes at the top surface of the sample was $\phi^{\mathrm{T}} = +1.25 \times 10^6\, h$ V; while, an electrical ground condition was applied to the nodes at the bottom surface, i.e., $\phi^{\mathrm{B}} = 0$. The potential difference between the two surfaces was set up to produce an electric field of magnitude 1.25 MV m^{-1} in the −3 direction. Exchanging the applied potentials would result in an electric field of the same magnitude in the +3 direction.

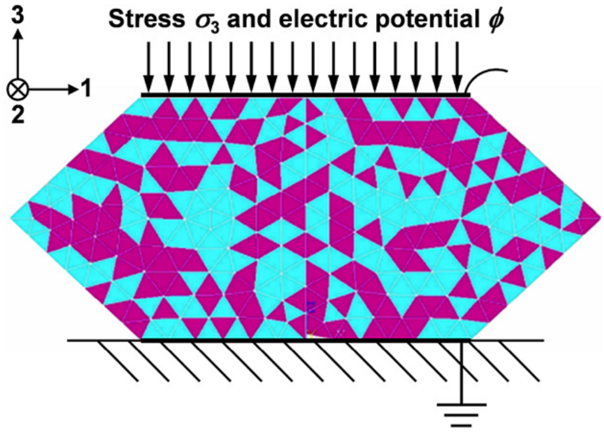

Figure 2. Mesh arrangement (average element edge length = 0.1 mm) and applied boundary conditions for a hexagonal prism $BaTiO_3$ single crystal sample for FE simulations. The type-II variant configuration is shown here, where blue elements are [100] variants and pink elements are [010] variants.

3. Results and discussion

3.1. Calculation of polarization and strain

The maximum possible variations in polarization and strain through 90° switching for the tetragonal $BaTiO_3$ single crystal, allowed by crystallography, are 0.26 C m^{-2} and 1.09%, respectively [15]. Experimental measurements close to these theoretical maximum values have been achieved by loading the crystal in the polar [001] direction [1, 5]. The loading arrangement shown in figure 1 indicates that when the $BaTiO_3$ single crystal (in the form of a hexagonal prism shape sample) is loaded in the [110] direction, polarization switching from one in-plane variant to another in-plane variant alone gives rise to no strain in the [110] direction; this is valid even for a non-180° switch (e.g., from [010] to [$\bar{1}$00] or from [100] to [0$\bar{1}$0]). Instead, a sizable strain in the [110] direction only becomes apparent when the out-of-plane variant is included in the switching path (e.g., from [010] to [001] and then to [$\bar{1}$00] or [0$\bar{1}$0], or other equivalent switching routes). Based on the crystal geometry and laboratory coordinate system defined in figure 1, the polarization $\bar{\boldsymbol{P}}$ and strain $\bar{\boldsymbol{\varepsilon}}$ associated with the ferroelectric variants under the hexagonal prism configuration are:

$$\bar{\boldsymbol{P}}^{[100],[\bar{1}00]} = \pm\frac{P_s}{\sqrt{2}}\begin{pmatrix}1\\0\\1\end{pmatrix} \quad \text{and}$$

$$\bar{\boldsymbol{\varepsilon}}^{[100],[\bar{1}00]} = \begin{pmatrix}\frac{\eta_1+\eta_2}{2} & 0 & \frac{\eta_1-\eta_2}{2}\\ 0 & \eta_2 & 0\\ \frac{\eta_1-\eta_2}{2} & 0 & \frac{\eta_1+\eta_2}{2}\end{pmatrix};$$

$$\bar{\boldsymbol{P}}^{[010],[0\bar{1}0]} = \pm\frac{P_s}{\sqrt{2}}\begin{pmatrix}-1\\0\\1\end{pmatrix} \quad \text{and}$$

$$\bar{\boldsymbol{\varepsilon}}^{[010],[0\bar{1}0]} = \begin{pmatrix}\frac{\eta_1+\eta_2}{2} & 0 & \frac{\eta_2-\eta_1}{2}\\ 0 & \eta_2 & 0\\ \frac{\eta_2-\eta_1}{2} & 0 & \frac{\eta_1+\eta_2}{2}\end{pmatrix};$$

$$\bar{\boldsymbol{P}}^{[00\bar{1}],[001]} = \pm P_s\begin{pmatrix}0\\1\\0\end{pmatrix} \quad \text{and}$$

$$\bar{\boldsymbol{\varepsilon}}^{[00\bar{1}],[001]} = \begin{pmatrix}\eta_2 & 0 & 0\\ 0 & \eta_1 & 0\\ 0 & 0 & \eta_2\end{pmatrix},$$

where P_s is the spontaneous polarization of tetragonal $BaTiO_3$ ($P_s = 0.26$ C m^{-2}), and η_1 and η_2 are the measured parameters for the spontaneous strain of tetragonal $BaTiO_3$ ($\eta_1 = 0.67\%$ and $\eta_2 = -0.42\%$) [15]. The maximum actuation strain in the [110] direction is achieved through an in-plane to out-of-plane (or vice versa) 90° switch, which is of an absolute value of $\frac{\eta_1+\eta_2}{2} - \eta_2 = \frac{\eta_1-\eta_2}{2} = 0.545\%$. For such a switch, the corresponding polarization change in the [110] direction is of an absolute value of $\frac{P_s}{\sqrt{2}} = 0.184$ C m^{-2}. The analytical calculation shows that for the tetragonal $BaTiO_3$ single crystal, the maximum possible switching strain in the non-polar [110] direction (0.545%) is half of that in the polar [001] direction (1.09%).

3.2. FE simulations

The FE simulations of the distributions of electric potential, stress and displacement vectors within the hexagonal prism shape $BaTiO_3$ single crystal sample under several representative loading and variant combinations are shown in figures 3 and 4. The two types of variant configurations constructed within the crystal sample—the presence of only the [001]/[00$\bar{1}$] variant pair and only the [100]/[010] variant pair—are designated 'type-I' and 'type-II' variant configurations, respectively, in the following discussion. It is evident that regardless of the loading and variant combination, the equipotential lines (surfaces) at the central portion of the hexagonal prism shape sample have relatively equal spacing and are parallel to the electrode surfaces (see figures 3(a)–(d)). This indicates the presence of a uniform strength electric field parallel to the laboratory 3-axis. In contrast, the electric field within the triangular flanks of the sample is highly non-uniform due to the effects of shape irregularity—the field direction is not constant and field strength is decreased at the acute corner. As for the distribution of stress, a relatively constant stress is predicted in the sample volume enclosed by the top and bottom electrodes, on which the mechanical loading is applied (see figures 3(e) and (f)). In comparison, the stress within the triangular flanks (not enclosed by the electrodes) is less uniform and of a magnitude smaller than that in the central region. Due to the edge effects, stress concentrations at the obtuse corners of the hexagonal prism shape sample are evident. For the type-II variant configuration, the *c*-axis of the tetragonal [100] and [010] variants is shortened and lengthened, respectively, by a large applied compressive stress and a large applied +3 direction electric field. Under such variant and loading combination, the restriction of piezoelectric expansion will result in the central portion of the crystal sample experiencing stresses significantly larger than the external applied stress (see figure 3(f)).

As for the distribution of displacement vectors, the combination of a large compressive stress, zero electric field and type-I variant configuration produces a large net displacement in the laboratory ±2 direction (see figure 4(a)); while, the combination of a large +3 direction electric field, zero compressive stress and type-II variant configuration, produces a large net displacement in the laboratory +3 direction (see figure 4(b)). For the type-II variant configuration, the *c*-axis of the tetragonal [100] and [010] variants is shortened by both the −3 direction electric field and large compressive stress. Under such a variant and loading combination, a large net displacement in the laboratory ±1 direction is predicted (see figure 4(c)). Notice that the FE simulations performed were static simulations, in which no ferroelectric or ferroelastic switching occurred within the crystal sample. The displacements are therefore induced by linear piezoelectricity and elasticity. The simulation results suggest that for the analysis of [110] electromechanical loading responses of $BaTiO_3$ single crystals, the utilization of a hexagonal prism shape crystal sample is a feasible approach, provided that the polarization and strain data are collected from the region within the sample where electric and stress fields are uniform. Such a requirement was met in this study by choosing strain gauges with a gauge width much shorter than the length of the electrodes (see figure 1). Further modeling investigations based on approaches that incorporate domain switching, e.g., those proposed by Tsou *et al* [6] and

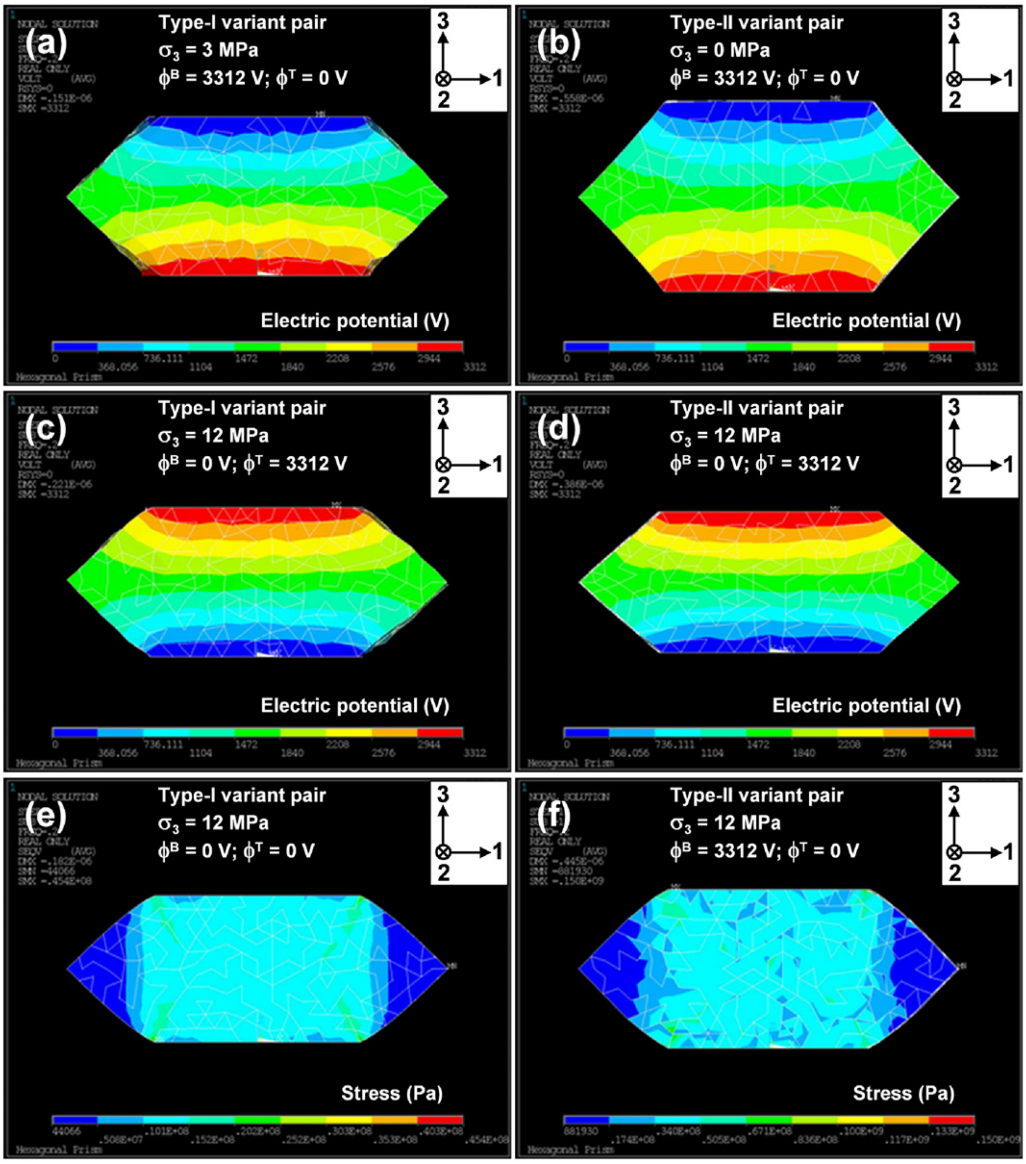

Figure 3. FE simulations of (a)–(d) distribution of electric potential and (e), (f) distribution of stress within a hexagonal prism $BaTiO_3$ single crystal sample under various loading and variant combinations. In each sub-figure, the type of variant configuration, applied compressive stress magnitude, and applied potentials on the top and bottom electrodes are indicated.

Lewis *et al* [16], should reveal more details on the strain actuation of the hexagonal prism shape crystal.

3.3. Loading responses at room temperature

The polarization and strain hysteresis curves for the (001)-oriented $BaTiO_3$ single crystal loaded and measured in the [110] direction at room temperature are shown in figures 5(a) and (b), respectively. The small offset in the measured strain hysteresis curves (i.e., left half versus right half; see figure 5(b)) is likely due to imperfect attachment of the strain gauge to the tiny hexagonal prism shape sample. It is evident that the polarizations produced at maximum electric field under bias stresses ranging from 0 to 3.0 MPa were close to 0.184 C m^{-2}, the theoretical polarization value for in-plane to out-of-plane (or vice versa) 90° switching (see calculation in section 3.1). However, the rapid and nonlinear decrease in polarization during electric field unloading, even in the absence of mechanical bias, proved that strong depolarization fields were present within the crystal, affecting the stability of the (near) single-domain state developed at maximum electric field. The small remanent polarization (P_r) was therefore the result of a highly nonlinear depolarization behavior. For the hexagonal prism crystal sample prepared for the [110] loading experiment, the total area of the unshielded surfaces (including two hexagonal side faces) is significantly larger than that of the electroded surfaces (see figure 1). Depolarization fields generated from the unshielded surfaces would effectively randomize the single-domain state during electric field unloading, resulting in domains of different variants, including the out-of-plane domains, at zero electric field. The appearance of out-of-plane [001] and/or [00$\bar{1}$]

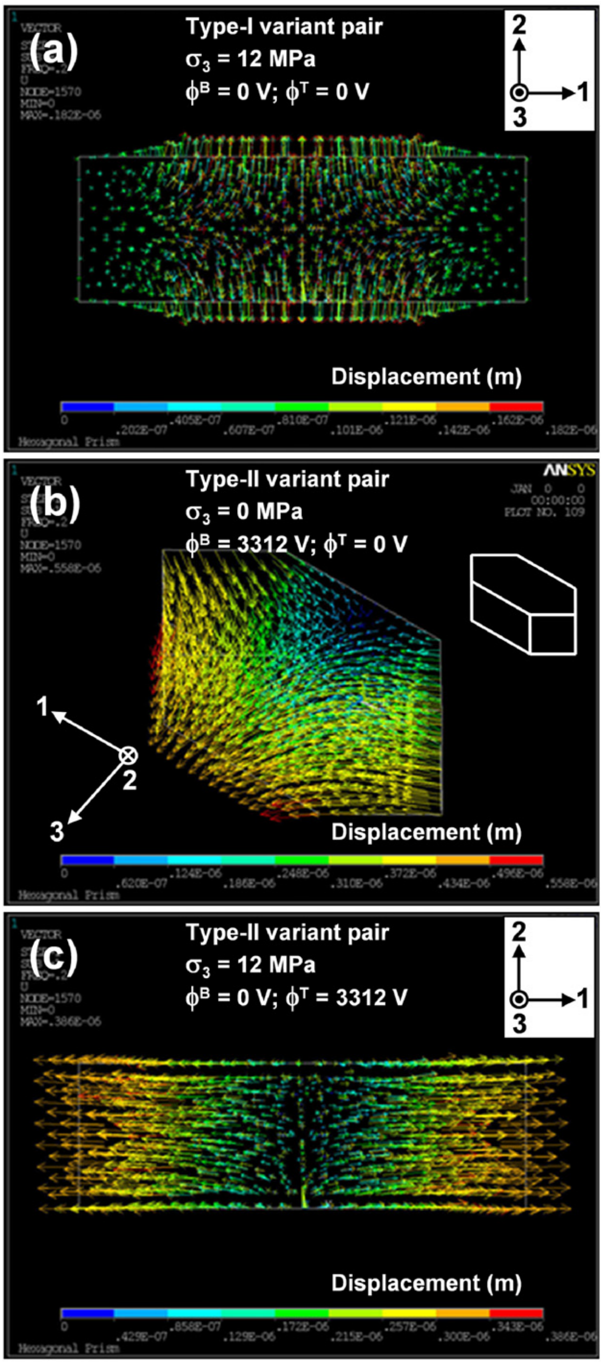

Figure 4. FE simulations of (a)–(c) distribution of displacement vectors within a hexagonal prism $BaTiO_3$ single crystal sample under various loading and variant combinations. In each sub-figure, the type of variant configuration, applied compressive stress magnitude, and applied potentials on the top and bottom electrodes are indicated.

domains during cyclic electrical loading, induced either from the depolarization phenomenon or by the bias stress-activated ferroelastic 90° switching, is essential to a large [110] electrostrain.

Figure 5(b) shows that the [110] electrostrain was promoted only slightly by the bias stress. When the bias stress was increased to 4.4 MPa, the cycling of the polarization between the in-plane and out-of-plane variants was constrained, resulting in a reduction of [110] electrostrain. The maximum [110] electrostrain produced from switching at room temperature (denoted as $\varepsilon_{[110],\mathrm{max,RT}}$, where the last term of the subscript describes the loading temperature) was 0.20% at 3.0 MPa (see figure 5(b)). In comparison, the authors showed previously that the maximum [001] electrostrain obtained from loading the MTI's (001)-oriented $5 \times 5 \times 2$ mm^3 cuboidal $BaTiO_3$ single crystal in the [001] direction at room temperature (denoted as $\varepsilon_{[001],\mathrm{max,RT}}$) was 0.45% at 2.7 MPa [4, 5]. The strain data from the loading experiments indicate that the ratio between $\varepsilon_{[110],\mathrm{max,RT}}$ and $\varepsilon_{[001],\mathrm{max,RT}}$ is 0.44, which is in reasonable agreement with the ratio predicted by the analytical calculation (0.5; see section 3.1). Moreover, $\varepsilon_{[110],\mathrm{max,RT}}$ and $\varepsilon_{[001],\mathrm{max,RT}}$ were induced at almost identical bias stress levels, and both only reached about 40% of their respective theoretical maximum values. This suggests that the $BaTiO_3$ single crystals used in our loading studies exhibited a relatively constant out-of-plane 90° switching coercivity at room temperature regardless of the loading direction.

Figure 5(b) shows that the [110] electrostrain produced from switching under pure electrical loading (i.e., zero bias stress) at room temperature (denoted as $\varepsilon_{[110],\mathrm{elec,RT}}$) was about 0.18%, a value surprisingly comparable to $\varepsilon_{[110],\mathrm{max,RT}}$ (0.20% at 3.0 MPa). The large $\varepsilon_{[110],\mathrm{elec,RT}}$ implies that even without the aid of the bias stress, the action of depolarization during electric field unloading alone can produce a large number of stable out-of-plane domains. This is believed to be ascribed to the combination of a relatively small out-of-plane 90° switching coercivity and a strong depolarization field in the out-of-plane direction, generated from the large unshielded hexagonal side faces of the hexagonal prism crystal sample. Preliminary experimental work based on the *in situ* domain observation and switching current analysis of MTI's $BaTiO_3$ single crystals under different switching conditions has revealed that the starting and finishing electric fields of out-of-plane 90° switching (0.05 and 0.25 MV m^{-1}, respectively) are considerably smaller than those of in-plane 90° and 180° switchings at room temperature. The large $\varepsilon_{[110],\mathrm{elec,RT}}$ indicates that at room temperature the out-of-plane variant is included in the switching path even in the absence of stress-activated ferroelastic switching, and in-plane to out-of-plane (or vice versa) 90° switching still dominates the overall switching behavior. An important conclusion can therefore be drawn: apart from the bias stress magnitude, the combined effect of the depolarization field and switching coercivity is another critical factor governing the strain actuation of $BaTiO_3$ single crystals.

It has been shown previously by the authors that the [001] electrostrain obtained from loading the MTI's (001)-oriented $5 \times 5 \times 2$ mm^3 cuboidal $BaTiO_3$ single crystal electrically in the [001] direction at room temperature (denoted as $\varepsilon_{[001],\mathrm{elec,RT}}$) was about 0.14% [4, 5], a value smaller than $\varepsilon_{[110],\mathrm{elec,RT}}$ (0.18%) measured in this study. Such a comparison indicates that the electrostrain of $BaTiO_3$ single crystals can be increased by depolarization fields which promote strain-inducing switching. This gives rise to the

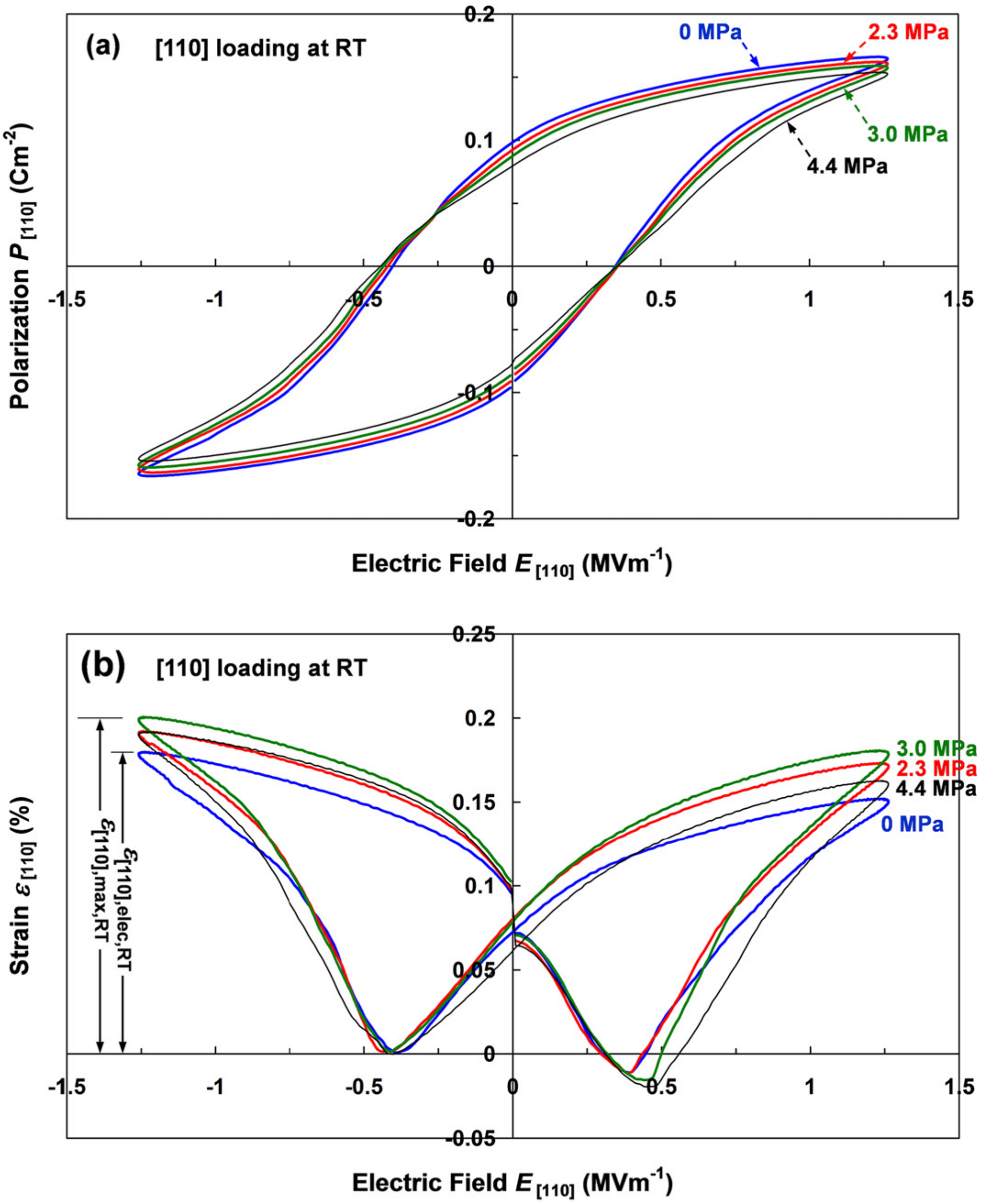

Figure 5. (a) Polarization and (b) strain hysteresis curves for a hexagonal prism $BaTiO_3$ single crystal loaded and measured in the [110] direction at room temperature.

notion that for the application of $BaTiO_3$ single crystals in high-strain actuator devices, if pre-stressing the crystal bulk via the device housing and/or proof mass is not attainable, an alternative approach for strain promotion could be to design a novel crystal bulk shape with specifically positioned electrodes, so that when under electric field excitation, the crystal would experience accompanying depolarization fields that promote strain-inducing switching.

3.4. Loading responses at 55 °C

The polarization and strain hysteresis curves for the (001)-oriented $BaTiO_3$ single crystal loaded and measured in the [110] direction at 55 °C are shown in figures 6(a) and (b), respectively. Again, the small offset in the measured strain hysteresis curves is likely due to imperfect attachment of the strain gauge. It is evident that the polarization hystereses were not fully developed at 55 °C and exhibited smaller saturation and remanent values compared to those measured at room temperature. This suggests that the hexagonal prism crystal sample became harder to switch and pole, and exhibited a higher degree of domain randomness at small electric fields when the loading temperature was increased to 55 °C. Preliminary experimental work has revealed that the starting electric field of in-plane 90° switching is decreased from 0.15 to 0.08 MV m^{-1} when the temperature is increased from room temperature to 55 °C. The measured polarization hystereses also indicate that the coercive field (E_c) of the crystal sample

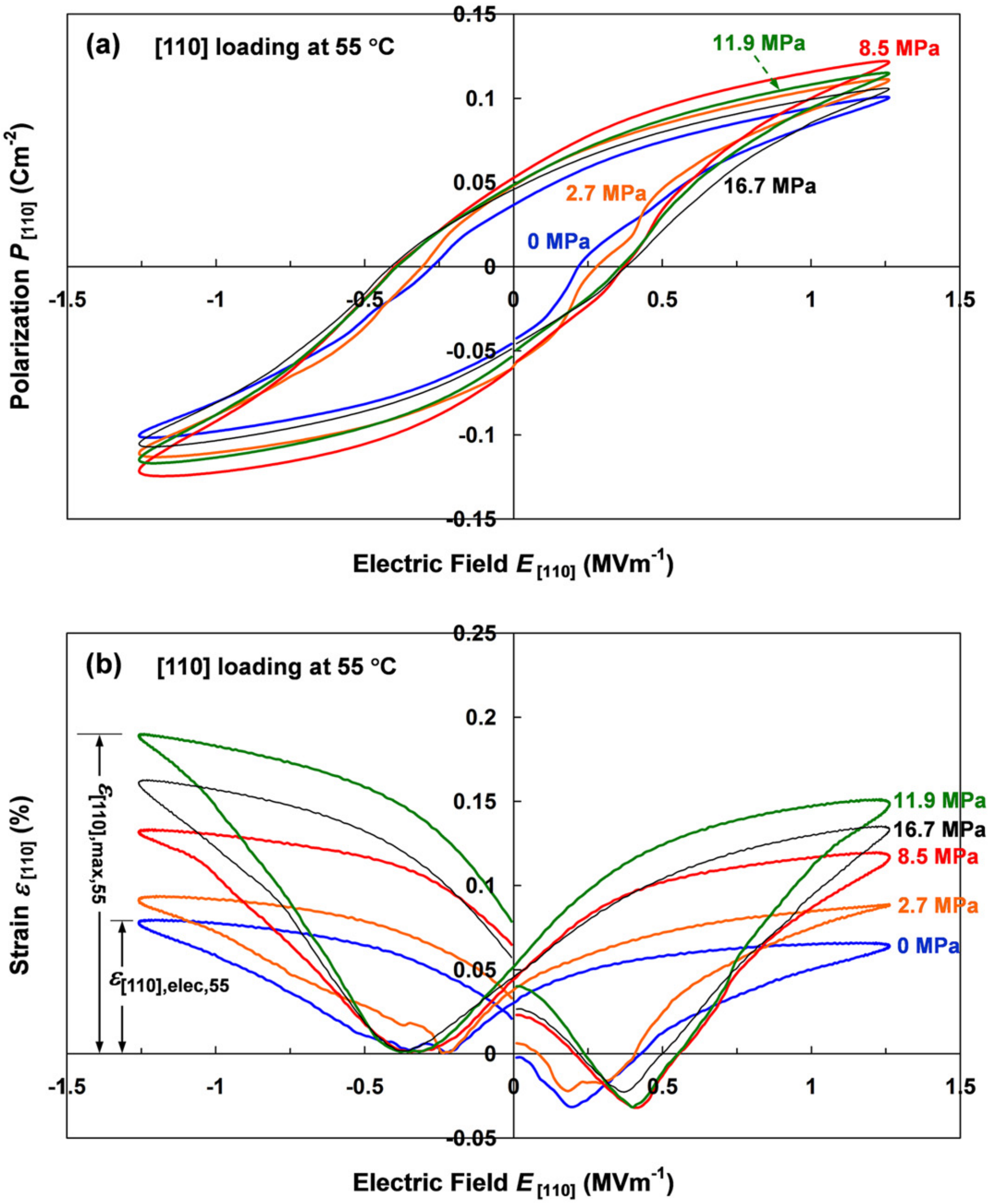

Figure 6. (a) Polarization and (b) strain hysteresis curves for a hexagonal prism $BaTiO_3$ single crystal loaded and measured in the [110] direction at 55 °C.

at zero or small bias stresses, which is a good indicator of the effective in-plane switching coercivity, is smaller at 55 °C (see figures 5(a) and 6(a)). Thus, due to the decrease of switching coercivities at 55 °C, especially those associated with in-plane switchings, the depolarization fields within the hexagonal prism shape sample became more effective in opposing the formation of a single-domain state at maximum electric field, as well as more effective in randomizing the domains during electric field unloading.

Figure 6(b) shows that the maximum [110] electrostrain produced from switching at 55 °C ($\varepsilon_{[110],\max,55}$) was 0.19% at 11.9 MPa. This maximum strain is similar to the maximum strain obtained at room temperature ($\varepsilon_{[110],\max,RT} = 0.20\%$ at 3.0 MPa), but was only achieved with a much larger bias stress. Due to the substantial decrease of in-plane switching coercivities at 55 °C, more domains would be randomized to the in-plane variant directions by the depolarization fields during electric field unloading. Hence, a much larger bias stress was required at 55 °C to override the depolarization effect and ferroelastically switch a sufficient number of domains to the out-of-plane variant directions at small electric fields, which would then be ferroelectrically switched back to the in-plane variant directions at high electric fields, resulting in [110] electrostrain. Figure 6(b) shows that the [110] electrostrain produced from switching under pure electrical loading at 55 °C ($\varepsilon_{[110],\mathrm{elec},55}$) was less than 0.1%, a value significantly smaller than $\varepsilon_{[110],\max,55}$. This is in contrast to the strain behavior observed at room temperature, where $\varepsilon_{[110],\mathrm{elec},RT}$ is comparable to $\varepsilon_{[110],\max,RT}$. Based on the notion that at 55 °C more domains are randomized to the

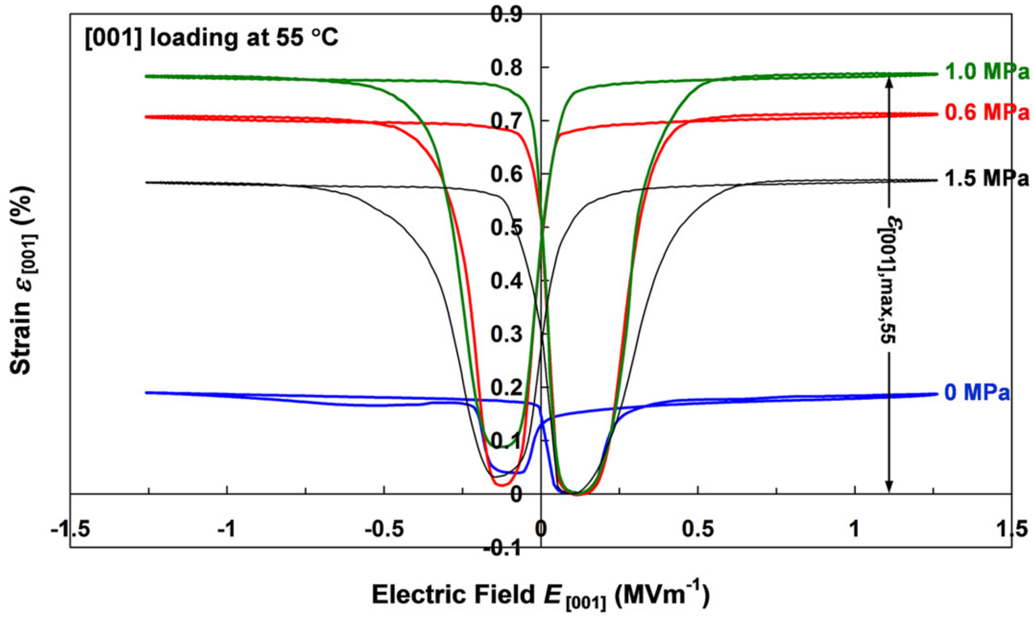

Figure 7. Strain hysteresis curves for a (001)-oriented cuboidal $BaTiO_3$ single crystal loaded and measured in the [001] direction at 55 °C [5].

in-plane variant directions during electric field unloading, it is expected that without the aid of a large bias stress, in-plane 90° and/or 180° switchings, which give rise to no [110] strain, would dominate the switching behavior during cyclic electrical loading. The small measured $\varepsilon_{[110],\mathrm{elec},55}$ ($<0.1\%$) provides the supporting evidence.

From the switching characteristics observed at 55 °C, it is clear that in order to effectively maximize the electrostrain of $BaTiO_3$ single crystals with a small bias stress, the promotion of non-strain-inducing switchings by the depolarization fields must be minimized. An optimal loading scenario for strain actuation is best demonstrated by the strain hysteresis of the MTI's (001)-oriented $5 \times 5 \times 2$ mm^3 cuboidal $BaTiO_3$ single crystal loaded and measured in the [001] direction at 55 °C (see figure 7) [5]. It is evident that when the depolarization effect within the crystal sample was minimized because of a small unshielded surface area (two major 5×5 mm^2 faces were electroded) and the switching coercivities were reduced at 55 °C, the cuboidal $BaTiO_3$ single crystal displayed the classic features of soft ferroelectricity and a large electrostrain was achieved with a tiny bias stress ($\varepsilon_{[001],\mathrm{max},55} = 0.8\%$ at 1.0 MPa). Of course loading and measuring in the polar [001] direction allowed the observation of the largest possible switching strain of the $BaTiO_3$ single crystal. An interesting further comparison study would be to investigate the electromechanical loading responses of (110)-oriented cuboidal $BaTiO_3$ single crystals with a small unshielded surface area (prepared by precision machining) in order to further elucidate the effects of depolarization and switching coercivity on the strain actuation of $BaTiO_3$ single crystals.

4. Conclusion

The switching characteristics of $BaTiO_3$ single crystals under uniaxial electromechanical loading in the non-polar [110] direction at room temperature and 55 °C have been investigated in this study. Experimentally, this was achieved by machining the (001)-oriented cuboidal crystal into a hexagonal prism by cutting off two opposite corners of the cuboid, and the resulting two parallel cut faces became the top and bottom electrode surfaces, allowing the application of electrical and mechanical loads parallel to the [110] direction. Polarization and strain hysteresis measurements in the [110] direction revealed that under the combination of large in-plane switching coercivities and a strong out-of-plane depolarization field, strain-inducing 90° in-plane to out-of-plane (or vice versa) switching was the dominant switching behavior even in the absence of mechanical bias. By lowering the in-plane switching coercivities, a contrasting non-strain-inducing behavior characterized by switching between the in-plane variants was observed. An important conclusion is drawn: apart from the bias stress magnitude, the combined effect of the depolarization field and switching coercivity is another critical factor governing the strain actuation of $BaTiO_3$ single crystals. The present study also reveals the possibility of increasing the strain capacity of $BaTiO_3$ single crystals by introducing accompanying depolarization fields which promote strain-inducing 90° switching. This approach could be potentially useful when bias stress-activated ferroelastic switching is not attainable.

Acknowledgments

The authors are grateful for the financial support of the National Science Council (NSC) of Taiwan R.O.C. under contract numbers 100-2628-E-002-024-MY2 and 100-2628-E-002-034-MY3 and the Office of Research and Development of National Taiwan University under contract number 102R7718.

References

[1] Burcsu E, Ravichandran G and Bhattacharya K 2004 Large electrostrictive actuation of barium titanate single crystals *J. Mech. Phys. Solids* **52** 823–46

[2] Yen J H, Shu Y C, Shieh J and Yeh J H 2008 A study of electromechanical switching in ferroelectric single crystals *J. Mech. Phys. Solids* **56** 2117–35

[3] Shu Y C, Yen J H, Shieh J and Yeh J H 2007 Effect of depolarization and coercivity on actuation strains due to domain switching in barium titanate *Appl. Phys. Lett.* **90** 172902

[4] Shieh J, Yeh J H, Shu Y C and Yen J H 2007 Operation of multiple 90° switching systems in barium titanate single crystals under electromechanical loading *Appl. Phys. Lett.* **91** 062901

[5] Shieh J, Lin J A and Shu Y C 2009 A temperature-dependent study on the polarization-free straining of barium titanate single crystals *Smart Mater. Struct.* **18** 104018

[6] Tsou N T, Potnis P R and Huber J E 2011 Classification of laminate domain patterns in ferroelectrics *Phys. Rev.* B **83** 184120

[7] Park S E and Shrout T R 1997 Ultrahigh strain and piezoelectric behavior in relaxor based ferroelectric single crystals *J. Appl. Phys.* **82** 1804–11

[8] Wada S, Suzuki S, Noma T, Suzuki T, Osada M, Kakihana M, Park S E, Cross L E and Shrout T R 1999 Enhanced piezoelectric property of barium titanate single crystals with engineered domain configurations *Japan. J. Appl. Phys.* I **38** 5505–11

[9] Liu T and Lynch C S 2003 Ferroelectric properties of [110], [001] and [111] poled relaxor single crystals: measurements and modeling *Acta Mater.* **51** 407–16

[10] Li J Y and Liu D 2004 On ferroelectric crystals with engineered domain configurations *J. Mech. Phys. Solids* **52** 1719–42

[11] Merz W J 1953 Double hysteresis loop of $BaTiO_3$ at the Curie point *Phys. Rev.* **91** 513–7

[12] Shieh J, Huber J E and Fleck N A 2003 An evaluation of switching criteria for ferroelectrics under stress and electric field *Acta Mater.* **51** 6123–37

[13] Berlincourt D and Jaffe H 1958 Elastic and piezoelectric coefficients of single-crystal barium titanate *Phys. Rev.* **111** 143–8

[14] Dent A C, Bowen C R, Stevens R, Cain M G and Stewart M 2007 Effective elastic properties for unpoled barium titanate *J. Eur. Ceram. Soc.* **27** 3739–43

[15] Jona F and Shirane G 1962 *Ferroelectric Crystals* (New York: Pergamon) pp 108–210

[16] Lewis R W C, Dent A C E, Stevens R and Bowen C R 2011 Microstructural modelling of the polarization and properties of porous ferroelectrics *Smart Mater. Struct.* **20** 085002